

# $H_{\alpha}$ measurements on hot-ion-mode plasmas in the minimum-B anchor cell of the GAMMA 10 tandem mirror

Y. Nakashima,<sup>a)</sup> S. Kobayashi, H. Aminaka, T. Fukasawa, M. Shoji,<sup>b)</sup> Y. Ishimoto, Y. Kubota, M. Yoshikawa, E. Kawamori, M. Ichimura, M. K. Islam, and K. Yatsu  
*Plasma Research Center, University of Tsukuba, Tsukuba-shi, Ibaraki 305-8577, Japan*

(Presented on 10 July 2002)

Results of  $H_{\alpha}$  measurement in the GAMMA 10 tandem mirror are described, with a particular focus on the behavior of neutrals in the anchor minimum-B region. Recently a set of  $H_{\alpha}$  line-emission detector arrays was designed and installed in the anchor-cell, where the shape of the magnetic flux tube becomes flat and the cross section of plasma is elongated elliptically. The detector consists of  $H_{\alpha}$  interference filter, optical fiber, and photomultiplier with magnetic shield, and is absolutely calibrated by using a standard lamp. In standard ion-cyclotron-range-of-frequency heated, hot-ion-mode plasmas, detailed measurements of  $H_{\alpha}$  line-emission from the central-cell to the anchor-cell were carried out, and the dependence of the  $H_{\alpha}$  intensity on the quantity of gas puffing was investigated. The characteristic behavior of neutrals in the nonaxisymmetric anchor-cell is also discussed, based on the result of neutral transport simulation. © 2003 American Institute of Physics. [DOI: 10.1063/1.1537441]

## I. INTRODUCTION

Neutral hydrogen behavior is an important subject to investigate recycling phenomena and to clarify the particle balance on magnetically confined plasmas. In the tandem mirror devices, measurement of  $H_{\alpha}$  line-emission from the plasmas is also important to evaluate particle and energy confinement for obtaining high  $\beta$  plasmas.<sup>1,2</sup> In the GAMMA 10 tandem mirror, neutral hydrogen density in the central-cell has been estimated by measuring spatial profiles of  $H_{\alpha}$  line-emission with absolutely calibrated  $H_{\alpha}$  detectors.<sup>2-4</sup> Absolute measurements of  $H_{\alpha}$  line-emission enable us to evaluate the neutral density based on the collisional-radiative model.<sup>5</sup> Recently, a set of detector arrays was newly designed and installed in the inner-transition region of the anchor-cell, where the shape of the magnetic flux tube becomes flat and the cross section of plasmas is elongated elliptically. In this region, the thickness of the plasma is the same order of the mean-free-path length of hydrogen molecules, and is much shorter than that of Franck-Condon neutrals. Furthermore, a narrow space between the plasmas boundary and the vacuum vessel wall (a few centimeters) may permit strong wall-plasmas interactions in the anchor transition region. Under these circumstances, the behavior of neutrals provides valuable information not only for the tandem mirror research but also for the edge plasma investigation in divertor configuration.

In order to evaluate the neutral density profile in the tandem mirror plasma, the DEGAS neutral transport simulation code<sup>6</sup> has been applied in the GAMMA 10 device.<sup>2-4</sup> The code has been modified to take into account of dissociative-excitation reactions of molecular hydrogen in

order to adapt the simulation to low density range.<sup>2,6</sup> In standard ion-cyclotron-range-of-frequency (ICRF)-heated hot-ion-mode plasmas,<sup>7</sup> detailed measurements of  $H_{\alpha}$  line-emission from the midplane of the central-cell to the outer-transition region of the anchor-cell was performed using the detector system just discussed. In this paper, we describe the temporal and spatial characteristics of  $H_{\alpha}$  line-emission and discuss the behavior of neutrals in the nonaxisymmetric anchor-cell, based on the result of neutral transport simulation.

## II. EXPERIMENTAL SETUP

### A. The GAMMA 10 device

Figure 1 shows the schematic view of the GAMMA 10 tandem mirror together with the location of the diagnostic systems related to this experiment. GAMMA 10 is an effectively axisymmetrized minimum-B anchored tandem mirror with thermal barrier at both end-mirrors.<sup>8-10</sup> The device consists of an axisymmetric central-mirror cell, anchor-cells with minimum-B configuration, and plug/barrier cells with axisymmetric mirrors. The length of the central-cell is 6 m, and both ends of the central-cell are connected to the anchor-cells through the mirror throat regions. The magnetic strength of the central-cell is normally 0.43 T and varies from 0.3 to 0.57 T. Initial plasmas of hydrogen is injected by two plasma guns from both ends. The main plasma is then started up with ICRF waves in the central-cell and the anchor-cell, together with hydrogen gas puffing. Seven gas puffers are installed in the central-cell, and most of them are located away from the resonance layer in order to avoid the charge-exchange loss of hot ions. One of the ICRF waves (RF1: 9.9 MHz) is used for magnetohydrodynamics stabilization of the whole plasma at the anchor-cell. Another wave (RF2: 6.3 MHz) is used for heating the central-cell ions by

<sup>a)</sup>Electronic mail: nakashima@prc.tsukuba.ac.jp

<sup>b)</sup>National Institute for Fusion Science, 322-6 Oroshi-cho, Toki, Gifu 509-5292, Japan.

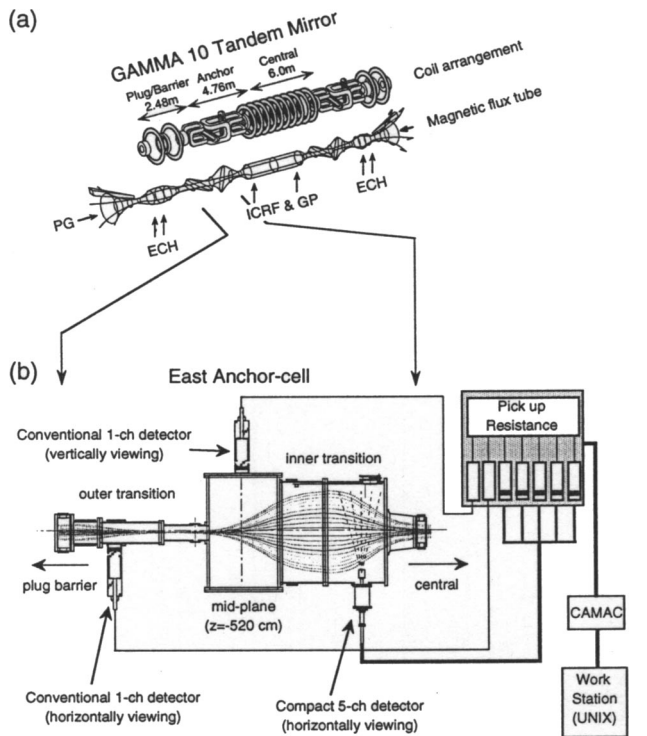


FIG. 1. The schematic view of GAMMA 10 and the location of the  $H_{\alpha}$  diagnostic system. (a) The GAMMA 10 coil system and the shape of the magnetic flux tube, together with the location of the plasma production and heating systems.

ion cyclotron resonance heating near the midplane of the central-cell, which is excited by a pair of the double half-turn antennas. The length of the plug/barrier cell is 2.5 m and the intensity of the magnetic field is 0.5 T at the midplane. The mirror ratio is 6.2 in this region. End-loss particles along the magnetic field lines are confined by the plug potential with electron-cyclotron heating in both plug/barrier cells.

### B. The $H_{\alpha}$ diagnostic system

Figure 2 shows the schematic view of  $H_{\alpha}$  line-emission detectors used in the present experiment. A conventional single-channel  $H_{\alpha}$  detector [Fig. 2(a)] consists of an  $H_{\alpha}$  interference filter (band width at full width at half maximum  $\Delta\lambda_{1/2}=2.7$  nm), a lens, and an optical fiber. In the east anchor-cell, as shown in Fig. 1(b), two sets of detectors of this type are installed on the midplane and on the outer-transition, respectively. A newly fabricated detector, shown in Fig. 2(b), which is a compact-type five-channel detector array, has individual lines of sights with different viewing angles by using five sets of bundled optical fiber cables. This detector is isolated from the vacuum with a view port 46 mm  $\phi$  in diameter and can be inserted into the vacuum vessel through the measuring port. The detector is also capable of rotating and moving along the insertion direction, which enables to measure the  $H_{\alpha}$  emission in a wide range of plasmas cross section of the inner-transition region of the anchor-cell, as shown in Fig. 1(b). All the detectors are absolute calibrated by using a standard lamp. The detected  $H_{\alpha}$  line-emission is transferred to magnetically shielded photomultiplier via optical fiber and the converted electric signal is then

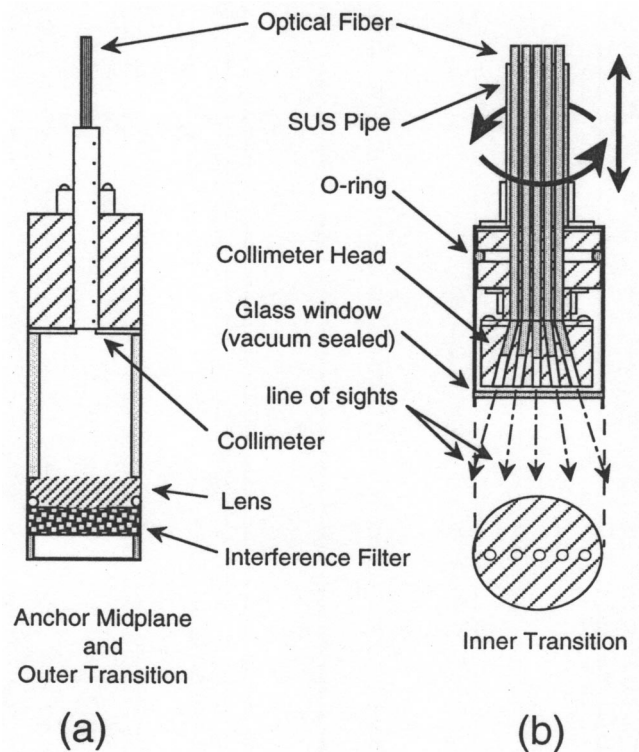


FIG. 2. Schematic view of  $H_{\alpha}$  line-emission detectors. (a) Conventional  $H_{\alpha}$  detector, (b) newly designed compact-type, 5-channel  $H_{\alpha}$  detector array.

moved to the CAMAC system, to be finally analyzed with a workstation. The profile of neutral density is determined with the help of a neutral transport simulation.

## III. EXPERIMENTAL RESULTS AND DISCUSSION

### A. Time behavior of $H_{\alpha}$ line-emission

In Fig. 3, a typical time behavior of plasma parameters and of  $H_{\alpha}$  line emission is shown in the ICRF-heated GAMMA 10 plasma. In this experiment, two types of gas puffers are used. One (GP#1b) is used for start-up of the plasma by injecting dense gas into the gas box ( $z=-240$  cm) with a short pulse. The other (GP#3a) is used for sustaining the plasma along with the ICRF pulse by continuously introducing gas in the mirror throat region ( $z=-300$  cm). Figure 3(b) shows the intensity of  $H_{\alpha}$  emission measured with the axial detector array of the central-cell and those measured at the gas box and the mirror throat. At the initial phase of plasma start-up, the signal at the gas box has a strong peak. This indicates that the influence of the gas puffer GP#1b is dominant in the initial phase of plasma start-up. In a steady-state phase, on the other hand, the  $H_{\alpha}$  intensity from the mirror throat is stronger than the other region, which implies that hydrogen atoms induced from GP#3a are localized in the vicinity of the mirror throat. The brightness of  $H_{\alpha}$  emission detected at the mirror throat is more than 10 times larger than that near the midplane.

In Fig. 3(c), the intensity of  $H_{\alpha}$  emission measured at the anchor-cell is shown. The observed peak in the initial phase also indicates the particle feed from the gas box and the

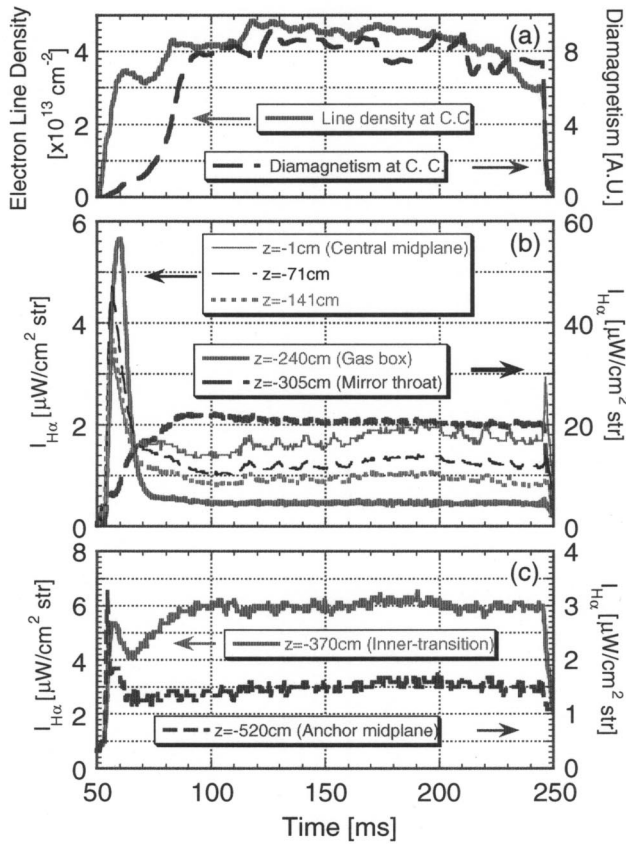


FIG. 3. Temporal behavior of the intensity in the  $H_{\alpha}$  emission measured in the region from the central-cell to the east anchor-cell, together with the line-density and diamagnetism at the central-cell. (a) Electron line-density and diamagnetism at the central-cell. (b)  $H_{\alpha}$  intensity measured at various positions in the central-cell. (c)  $H_{\alpha}$  intensity in the anchor-cell.

plasma production in the anchor-cell by the RF1 wave. After 80 ms, the time behavior of  $H_{\alpha}$  emission observed at the inner-transition region is different from that measured at the anchor midplane. The time behavior in the inner-transition is similar to that of the mirror throat. The explanation for these characteristics may be that the plasma escaping from the mirror throat can smoothly flow into the transition region, since there is no particle-trapping function in this region. On the other hand, the observation that the signal in anchor midplane resembles that of the central-cell, is ascribed to the mechanism that the passing particles in the anchor midplane are heated and trapped in the resonance area of RF1, which has the same as the central midplane.<sup>11</sup>

**B. Dependence of gas influx**

Figure 4 shows the dependence of  $H_{\alpha}$  intensity normalized by the electron line-density on the quantity of gas puffing. The  $H_{\alpha}$  intensity signals measured at the mirror throat and the inner-transition have a strong dependence on the reservoir pressure of GP#3. While the  $H_{\alpha}$  intensity at anchor midplane has no correlation with the pressure and normalized value with the line-density of anchor midplane is found to indicate a negative correlation. This implies that the hydrogen gas supplied from the mirror throat can reach the inner-transition region, while these gas molecules do not eas-

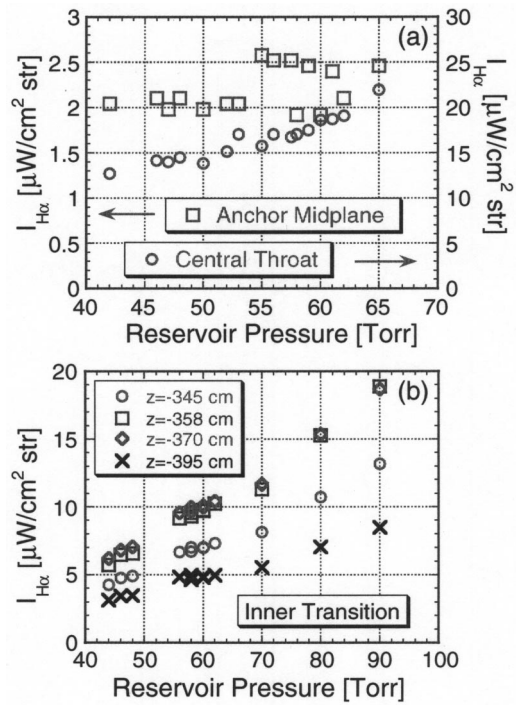


FIG. 4. Dependence of reservoir pressure of gas puffer at the mirror throat (#3) on  $H_{\alpha}$  signals measured at various positions.

ily arrive at the anchor midplane. From these results, a possible explanation of fueling to the anchor midplane is that most of the fueled particles are ionized near the mirror throat, pass through the inner-transition region, and are finally trapped with the resonant heating by an ICRF wave in the anchor midplane area.

**C. Axial profile of  $H_{\alpha}$  intensity in the inner-transition region**

The  $H_{\alpha}$  detector installed at the inner-transition has a compact style and is capable of measuring spatial distribution of the intensity by inserting the detector into the vacuum vessel of GAMMA 10. By changing the insertion length of the detector, the intensity profile of the  $H_{\alpha}$  signal was precisely measured along the magnetic field line in the east inner-transition. In this measurement, the volume of viewing plasma varies considerably with the measuring position on the axial direction. In order to correct this effect on the evaluation of axial distribution, we assume the radial profile of the plasma in this region to be Gaussian, and determine its  $1/e$  length based on the measured  $H_{\alpha}$  intensity.

Open circles in Fig. 5 show the data of  $H_{\alpha}$  intensity converted into the value on the line-of-sight, viewing the plasma axis by using the radial distribution of the measured  $H_{\alpha}$  signal. It is found that the  $H_{\alpha}$  intensity increases with the measured location being close to the anchor midplane. The solid curve in the figure represents the length of longer axis of the plasma cross section, which is almost equivalent to the plasma thickness along the line of sight. Measured data varies in correspondence with the curve, which indicates that the increase of  $H_{\alpha}$  intensity is ascribed to the increase of integration length in the viewing area of plasma cross sec-

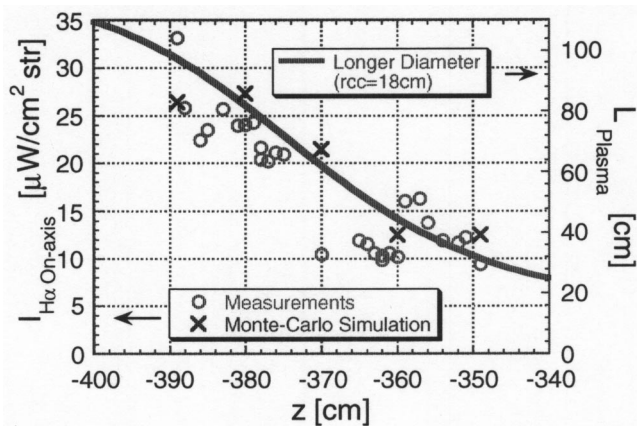


FIG. 5. Axial profile of  $H_{\alpha}$  intensity measured in the east inner-transition region and comparison with the simulation result. Circle is the measured result, cross represents the simulation results, and the solid curve shows the length of the longer axis of the plasma cross section.

tion. This result also implies that hydrogen molecules easily penetrate into the plasma from the direction of shorter axis of the plasma with an elliptic cross section, and make up a uniform neutral density profile. The “cross” symbol shows the predicted  $H_{\alpha}$  intensity from the two-dimensional (2D) Monte Carlo simulation, taking the shape of the plasma cross section at each axial position into consideration. Each calculated value is determined assuming that the molecular density is constant at the plasma boundary in every axial position. A good agreement between the measured results and those of the simulation shows the effectiveness of 2D Monte Carlo simulation on the prediction of neutral behavior in the anchor transition region, where the plasma cross section is flatly elongated. In near future, a fully three-dimensional simulation will provide more precise interpretation of experimental results and much detailed evaluation of neutral behavior in this region.

#### IV. SUMMARY

Detailed measurements of  $H_{\alpha}$  line-emission have been performed in the GAMMA 10 anchor-cell with nonaxisymmetric configuration of the magnetic field. A compact-type five-channel  $H_{\alpha}$  detector was designed and installed at the inner-transition region of the east anchor-cell with a highly elliptic plasma cross section. The dependence of the  $H_{\alpha}$  signal on the influx of gas puffing showed that the hydrogen molecules supplied from the mirror throat gas puffer can reach the inner-transition region, while these gas molecules do not easily arrive at the anchor midplane. An evaluation method for neutral particle behavior in the plasma with elliptic cross section of the nonaxisymmetric region, such as an anchor-cell, is successfully established by using the  $H_{\alpha}$  measurements with the help of a neutral transport simulation.

#### ACKNOWLEDGMENTS

The authors would like to acknowledge the members of the GAMMA 10 group, University of Tsukuba, for their collaboration in the experiments. Neutral transport simulation with the DEGAS code was carried out by a NEC SX-5 system at National Institute for Fusion Science Computer Center.

- <sup>1</sup>S. A. Allen *et al.*, Nucl. Fusion **27**, 2139 (1987).
- <sup>2</sup>Y. Nakashima *et al.*, J. Nucl. Mater. **196–198**, 493 (1992).
- <sup>3</sup>Y. Nakashima *et al.*, J. Nucl. Mater. **241–243**, 1011 (1997).
- <sup>4</sup>S. Kobayashi *et al.*, J. Nucl. Mater. **266–269**, 566 (1999).
- <sup>5</sup>L. C. Johnson and E. Hinnov, J. Quant. Spectrosc. Radiat. Transf. **13**, 333 (1973).
- <sup>6</sup>D. Hefietz, D. Post, and M. Petravic *et al.*, J. Comput. Phys. **46**, 309 (1982).
- <sup>7</sup>R. K. Janev, W. D. Langer, K. Evans, Jr., and D. E. Post, Jr., *Elementary Processes in Hydrogen-Helium Plasmas* (Springer, Berlin, 1987).
- <sup>8</sup>T. Tamano, Phys. Plasmas **2**, 2321 (1995).
- <sup>9</sup>M. Inutake *et al.*, Phys. Rev. Lett. **55**, 939 (1985).
- <sup>10</sup>K. Yatsu *et al.*, Nucl. Fusion **41**, 613 (2001).
- <sup>11</sup>M. Ichimura *et al.*, Nucl. Fusion **28**, 799 (1988).